International Journal of Engineering &Technology, 7 (4) (2018) 6768-6777

International Journal of Engineering & Technology

Website: www.sciencepubco.com/index.php/IJET
doi: 10.14419/ijet.v7i4.23870
Research paper

Formability characterization of aluminium AA6082-O sheet metal by uniaxial tension and Erichsen cupping tests

Eliaser T. Nghishiyeleke [1, 3], Melvin M. Mashingaidze [2] *, Adedayo A. Ogunmokun [1]

[1] *Mechanical and Industrial Engineering Department, University of Namibia*
[2] *Mining and Metallurgical Engineering Department, University of Namibia*
[3] *Power System Development, NamPower*
**Corresponding author E-mail: mmashingaidze@unam.na*

Abstract

AA6082 is a relatively new structural alloy in the 6000 aluminium alloy series. This study evaluated the deep drawability of AA6082-O sheet metal. Uniaxial Tensile tests were conducted on specimens prepared according to DIN 50125-E standard, for three angular orientations (0^0, 45^0, and 90^0) relative to the rolling direction. Erichsen Cupping tests were conducted on 60 mm × 60 mm blanks of two gauge thicknesses (1.0 mm and 2.0 mm) and also on segmented blanks. A WP 300 Universal Material Tester, with a loading capacity of 20 kN, was used for all the tests. The Tensile Strength was higher in the rolling direction (0^0) than in the transverse orientations (45^0 and 90^0). The resultant Forming Limit Curve (FLC) level of the established Forming Limit Diagrams (FLDs) was higher for the 2.0 mm thick blanks than the 1.0 mm thick blanks. Thus the alloy's formability is affected by the sheet thickness and orientation. It increases with sheet thickness, but the alloy exhibits planar anisotropy ($\Delta r<0$). AA6082 sheet fractures with no observable necking under uniaxial tension conditions, and exhibits non-uniform yielding characteristics. However, the general stress-strain behaviour is typical of that of the aluminium 6000 alloy series.

Keywords: *Aluminium AA6082-O Sheet Metal; Erichsen Cupping Test; Formability, Forming Limit Diagrams; Uniaxial Tensile Test.*

1. Introduction

Formability is the ability of the sheet metal to undergo plastic deformation prior to the onset of failure [1 - 3]. Regardless of the type of forming operation; the intrinsic and extrinsic characteristics of the sheet material, angular orientation relative to the sheet metal's rolling direction, and sheet thickness greatly influence the material's formability [3 - 5]. Unexpected failures may be encountered during the forming process; due to strain localization, poor surface finish or other defects of which the causes remain unknown [3], [6]. Moreover, little is known of material behaviour between the necking and rupture zones. In many cases the actual stampings are formed way beyond the necking point [7]. Little information is available on the formability of aluminium AA6082-O alloy; which is a relatively new structural alloy in the 6000 series aluminium alloys.

In this study the formability of AA6082-O alloy has been experimentally determined by Uniaxial Tension tests and Erichsen Cupping tests. Test specimens of two different gauge thicknesses (1.0 mm and 2.0 mm) were tested, using a WP 300 Universal Material Tester with a loading capacity of 20 kN.

1.1. AA6082-O alloy composition and mechanical properties

Aluminium AA6082-O alloy is a 6000-series variant, supplied in annealed (O) condition [8]. Like any other aluminium alloys in the 6000 series, magnesium and silicon are the major alloying elements for this alloy. The strength is moderate and attainable by heat treatment or cold working. The magnesium and silicon form the intermetallic compound; magnesium silicide, Mg_2Si, rendering the alloys heat-treatable. The alloy's typical composition is as listed in Table **1**:

Table 1: Typical AA6082-O Alloy Composition

Element	% by Weight
Aluminium (Al)	95.2 - 98.3
Silicon (Si)	0.7 - 1.30
Magnesium (Mg)	0.6 - 1.20
Manganese (Mn)	0.4 - 1.00
Iron (Fe)	0.0 - 0.50
Chromium (Cr)	0.0 - 0.25
Zinc (Zn)	0.0 - 0.20
Titanium (Ti)	0.0 - 0.10
Copper (Cu)	0.0 - 0.10
Residuals (Others)	0.0 - 0.15

Aluminium AA6082-O is a medium strength structural alloy, with excellent corrosion resistance, commonly used for machining in plate form. It has the highest ductility compared to any other AA6082 variants, and the highest tensile strengths of the 6000 series [8, 9]. The typical mechanical properties are given in Table **2** [8]:

Table 2: Typical Mechanical Properties of AA6082-O

Properties	Value
Proof Stress	85 MPa
Tensile Strength	140 MPa
Young's Modulus	69 GPa
Brinell Hardness	40 HB
Total Elongation at break	18 %

Copyright ©2018 Eliaser T. Nghishiyeleke et al. This is an open access article distributed under the Creative Commons Attribution License, which permits unrestricted use, distribution, and reproduction in any medium, provided the original work is properly cited.

As a relatively new alloy, with higher strength and excellent corrosion resistance compared to AA6061 alloy, AA6082-O alloy has replaced AA6061 in many applications; such as in the automotive industry, the aircraft industry and even in the ship building industry.

1.2. Structural sheet metals' formability characterization metrology

Formability evaluation of sheet metals involves measurement of strength, ductility, and the amount of deformation required prior to fracture. These parameters are normally experimentally determined, through mechanical simulative test experiments, to simulate the functional loads and conditions found in many formed sheet metal parts. In this study two simulative tests, relating to the strain hardening (n – value) in biaxial stretching and to the plastic anisotropy (r – value) in deep drawing operation were considered.

1.2.1. Formability characterization by uniaxial tensile test

The uniaxial tensile test is a mechanical simulative test method which involves pulling the specimen to failure in uniaxial tension conditions at a controlled slow strain rate while the specimen is in the test environment, and examining the specimen for evidence of stress-corrosion cracking [10]. The test is used to evaluate the formability of a given sheet metal in stretch forming operations, under uniaxial loading. This test technique can also be used to evaluate a new material, based on a general knowledge of formable sheet metals.

However, most structural metallic materials are anisotropic. The manner in which a metal sheet is processed and its thickness properties influence the uniformity of microstructure along the length of the test material. The location from which a test specimen is machined from the rolled metal sheet also influences the measured tensile properties.

Moreover, mechanical properties of the same sheet metal grade and thickness may vary from coil to coil, subsequently affecting the part quality and scrap rate, stress state and material flow (formability) [3]. These variations can be due to the directionality in the microstructure (texture) from forming or cold working operation, the controlled alignment of fibre reinforcement and a combination of a variety of other causes. Even in carefully performed test experiments, variations in tensile properties are always encountered.

Thus, formability determination of sheet metals by tensile tests is normally realised with test specimens machined in three principal angular orientations (0^0, 45^0 and 90^0, relative to the metal sheet rolling direction) as illustrated in Fig. 1.

Based on sheet metal formability literature [1], [11 - 15], the common fundamental metal sheet's formability characterization parameters in stretch forming, determined by tensile tests includes; the tensile strength; ductility, strain hardening exponent (n-value) and the plastic strain ratio (r-value).

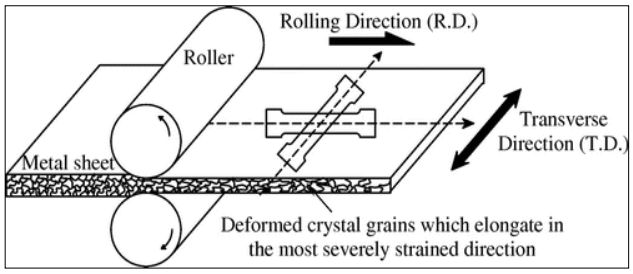


Fig. 1: Uniaxial Tensile Test Specimen Cut at an Angle of Orientation Relative to the Metal Sheet's Rolling Direction [16].

1.2.2. Total elongation, (% El)

The total elongation determines the capability of the sheet metal to stretch without necking and failure (ductility) [3], [11]. It is the ratio of the change in length (Δl) to the initial gauge length (l_o) of a tensile test specimen:

$$(\%El) = 100 \times \left(\frac{\Delta l}{l_o}\right) \quad (1)$$

A metal with a higher uniform elongation has the capability to undergo a large amount of strain hardening, hence a good formability.

1.2.3. Strain hardening exponent (n-value)

The n-value relates to the ability of a sheet material to undergo large uniform strains and plastic deformation during biaxial stretching [11], [16]. A high n-value indicates a large uniform elongation. The higher the n-value the better the formability of an alloy [10]. The n-value is determined by measuring the stress – strain response in the plastic region prior to necking [13], as described by the Holloman-Ludwig equation:

$$\sigma = K\varepsilon^n \quad (2)$$

Where σ, Ɛ, and K are the true stress, true strain and strength coefficient, respectively.

Graphically, the n-value is equivalent to the slope of the true stress/true strain curve up to the maximum load, when plotted on log-log coordinates [3], [14].

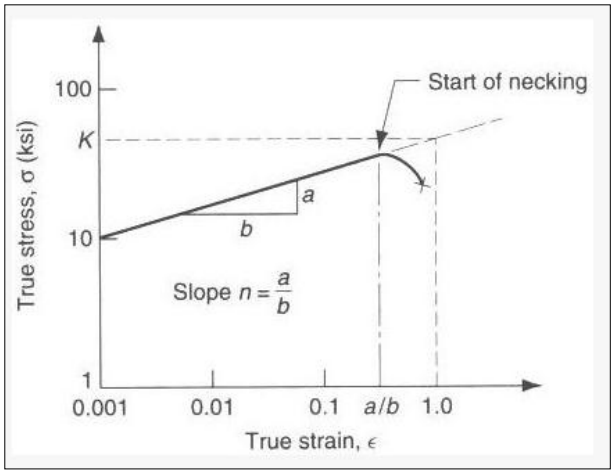


Fig. 2: Log True Stress-Log True Strain Curve [17].

The range of n-value is normally known to be $0 \leq n \leq 1$. The materials with $n = 0$ and $n = 1$ are said to be perfect plastic solid materials and elastic solid materials, respectively. However, ductile metals such as aluminium, normally exhibits n-value in narrow ranges ($0.02 \leq n \leq 0.5$) at room temperature [3].

1.2.4. Plastic strain ratio (r-value)

The plastic strain ratio measures sheet metal's drawability. It is useful for evaluating materials intended for forming shapes by deep drawing operations. The r-value is the ratio of the true width strain (ε_w) to the true thickness strain (ε_t) in sheet metal tensile testing [5], governed by ASTM E517 standard:

$$r = \frac{\varepsilon_w}{\varepsilon_t} = \frac{\ln \frac{w_o}{w_f}}{\ln \frac{l_f w_f}{l_o w_o}} \quad (3)$$

The subscripts o and f refer to the original and final dimensions of the specimen, respectively. The final length (l_f) and width (w_f) of a test specimen are measured at elongations below necking point. A high r-value ($r > 1$) is an indication of good drawing properties [15], [17]. The r-values for aluminium alloys, produced by con-

ventional rolling and annealing processes, are known to exist only in a narrow range ($0.55 < r < 0.85$).
The r-value is influenced by the sheet thickness and angular orientation of the test material relative to the rolling direction of the sheet. Hence, r-values are usually determined from three different angular direction of loading in the plane of sheet metal; (0^o, 45^o, and 90^o, relative to the rolling direction), and the normal r-value is taken to be the average. There are two types of plastic anisotropy, namely:

1) Planar anisotropy: The sheet material's properties in the thickness direction and in the plane of the sheet are different.
2) Normal anisotropy: The sheet material's properties vary with direction in the plane of the sheet.

1.2.5. Planar anisotropy (Δr-value)

The Δr-value determines the drawability of sheet metal in relation to the formation of ears on deep drawn parts [3].

$$\Delta r = \frac{r_{0^o} - 2r_{45^o} + r_{90^o}}{2} \quad (4)$$

The Δr-values are characteristically ≤ 0. When Δr = 0, no ears form on the drawn part. The height of the ears increases with Δr-values.

1.2.6. Average normal anisotropy (ravg-value)

The r_{avg}-value determines the limiting drawing ratio (drawability) of a drawn cup [3]. Using tensile test results the r_{avg}-value is determined as:

$$r_{avg} = \frac{r_{0^o} + 2r_{45^o} + r_{90^o}}{4} \quad (5)$$

Normally $0.4 \leq r_{avg} \leq 1.8$ [18], but aluminium alloys are known to have typical r_{avg}-values of $0.6 \leq r_{avg} \leq 0.8$. The formability of sheet metals increases with high r_{avg}-values [14], [18]. To have a better formability r_{avg} should exceed unity.
To optimise the deep drawability in sheet metal forming, a combination of high r_{avg} and low Δr-values is required [3, 19, 20]. In this case, the sheet metal is expected to have a low yielding strength, and high ductility.

1.2.7. Formability characterization by Erichsen cupping test

The Erichsen Cupping test is a mechanical simulative test method used to assess the ductility and determine the stretching properties of sheet metals [10], standardized by ISO 20482. The test consist of stretching the specimen, clamped at its edges between a blank holder and a die, into the circular form die cavity using a hemispherical punch until a through crack appears [3], [14], Fig. 3, and measuring the maximum depth of the impression at fracture.

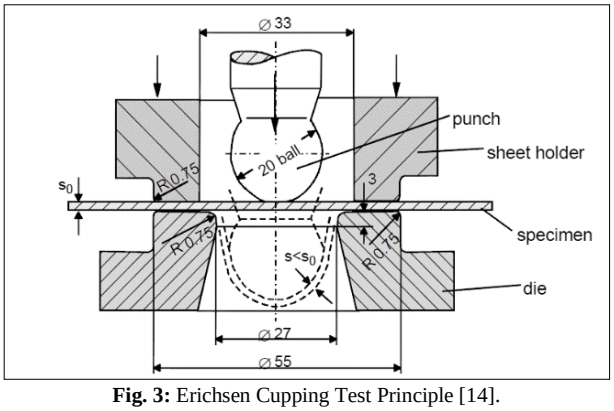


Fig. 3: Erichsen Cupping Test Principle [14].

This testing method is normally used to evaluate the formability of sheet metals and strips having a thickness of 0.1 mm up to 2 mm and a width of 90 mm or greater in stretch forming [21]. However, numerous test tool sets have also been developed, for cases when test materials are thicker and when only narrower strips are available [21].
A grid pattern of circles is printed on the surface of the test material, using electrochemical or photo printing technique prior to undertaking the deep drawing operation. The diameter (d_0) of these circles has a typical range of $2.5 \leq d_0 \leq 5.5$ mm. However, to improve the accuracy of measurements these circles could be made smaller as is practical.
Some of the printed circles deform into elliptical shapes of different sizes when subjected to loading. The dimensions of the deformed circles are used to determine the magnitude and direction of surface strains in sheet metal forming [3]. The depth of the formed indentation and diameters of the deformed circles are measured to determine the formability of the sheet material.
Based on deep drawing operations literature [3], [6], [7], [14], [21], [22], the most common formability indicative parameter of sheet metals in stretch forming by Erichsen Cupping test include: the Erichsen Index number (IE); the Limit Drawing Ratio (LDR); and Forming Limit Diagrams (FLDs).

1.2.8. Erichsen index number

The Erichsen Index number (IE) is equivalent to the depth of the drawn cup (punch penetration depth, h), measured upon the completion of the test [3]:

$$IE = \text{Punch penetration depth } (h) \quad (6)$$

Greater IE-values signify better formability.

1.2.9. Limit drawing ratio, LDR-value

The LDR-value measures the drawability of a sheet metal. It is the ratio of the maximum blank diameter (D_b) that can be drawn without tearing or failure to the smallest diameter of the cup drawn from the blank, represented by the punch diameter (D_p) [3], [10]:

$$LDR = \frac{D_b}{D_p} \quad (7)$$

The validity of the determined LDR value is subject to equation (8):

$$ln\left(\frac{D_0}{D_p}\right) \leq 1 \quad (8)$$

Theoretically, the maximum LDR value of a sheet metal in deep drawing operation could be as higher as 2.72. However, practically, due to friction and the effects of bending and unbending, the LDR is significantly lower than 2.72 [19]. The typical values of friction and tooling geometry LDR is in the range of $1.9 \leq LDR \leq 2.2$. The greater the LDR-value, the more extreme the amount of deep drawing. In mechanical deep drawing operations, an $LDR \geq 2$ signifies better formability [3].

1.3. Forming limits

Forming limit strains are used to determine the maximum multiaxial ductility of sheet metals [3]. The change in forming limits is determined experimentally using different specimen geometries and deformations with linear strain paths. Strains (major strain, ε_1 and minor strain, ε_2) can be evaluated from the deformation of circle grids, plotted on the surface of the test specimen upon unloading as illustrated in Fig. 4.

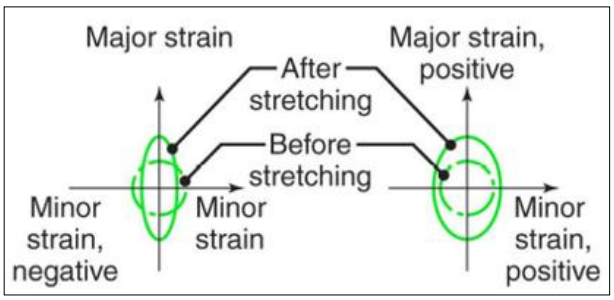


Fig. 4: Strain Analysis (Major and Minor Strain Determination).

1.3.1. Major Strain, ε1

The ε_2-value is determined from the largest dimension of the deformed circle (d_1: major axis of the formed ellipses), relative to the initial circle diameter (d_0):

$$\varepsilon_1 = \left(\frac{d_1 - d_0}{d_0}\right) \times 100 = \ln\left(\frac{d_1}{d_0}\right) \quad (8)$$

1.3.2. Minor Strain, ε2

The ε_2-value is determined from the smallest dimension of the deformed circle (d_2: minor axis of the formed ellipses), relative to the initial circle diameter (d_0):

$$\varepsilon_2 = \left(\frac{d_2 - d_0}{d_0}\right) \times 100 = \ln\left(\frac{d_2}{d_0}\right) \quad (10)$$

The pairs of the major strains and minor strains are used to determine the coordinates on the Forming Limit Curves (FLCs), and in the establishment of the Forming Limit Diagrams (FLDs).

1.3.3. Forming limit diagrams (FLDs)

The FLDs (Fig. 5) are the traditional failure prediction tool, used for the formability characterization of sheet metal under uniaxial, biaxial, and equal-biaxial tension conditions, proposed by Keeler (1965) and Goodwin (1968) [3], [14], [23], [15].

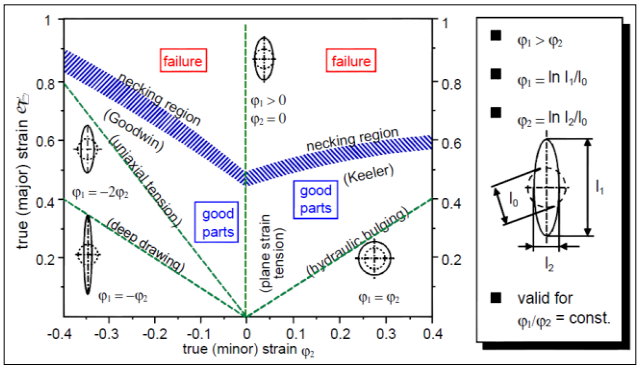


Fig. 5: Typical FLD Schematic by Keeler and Goodwin [14].

The diagram is established by plotting the major strains at the onset of necking of a sheet metal on the vertical axis and the corresponding minor strains on the horizontal axis [10]. The onset-of the failure line (Forming Limit Curve - FLC) divides all possible strain combinations into two zones: the safe zone (in which failure during forming is not expected) and the failure zone (in which failure during forming is expected). Numerous studies [14, 23-34] indicate that Forming Limit Diagrams are effective tools for measuring the formability of sheet metals. However, the forming limits are affected by punch arc radii, condition of the sheet metal, material properties (e.g. tensile strength), strain condition in geometrical features of the sheet metal, and thickness of the sheet metal. Every sheet metal has a unique Forming Limit Diagram defining its formability, strain limit, and the forming regions [31]. A formability study on steel sheets by [32] confirmed that the strain rate has a significant influence on the formability of steel sheets as exemplified by high strain rate FLC being lower than the static strain rate FLC in the biaxial stretch forming region.

2. Materials and methods

2.1. Uniaxial tensile test experiment

Two sets of AA6082-O rectangular cross-section, flat specimens (1.0 mm and 2.0 mm, with 9 specimens per thickness) were prepared. These specimens were machined according to DIN 50125 Standard Shape E. The specimens were cut at three angular orientations (0^0, 45^0 and 90^0, relative to the metal sheet rolling direction), and a total of 3 specimens per orientation were used. The contour of the sections of the specimens complied with DIN 50125 - E8 Standard (see Fig. 6-7).

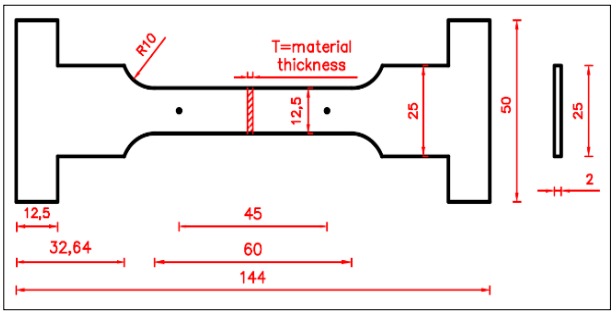


Fig. 6: Rectangular Cross-Section Tensile Test Specimen.



Fig. 7: Tensile Test Specimen Samples.

A WP 300 Universal Material Tester, with a loading capacity of 20 kN, fitted with an extensometer and a computerised data acquisition system was used to carry out the experiments.
The test setup was established on the tensile zone of the Universal Material Tester. The specimens were then subjected to tensional load slowly and continuously until fractured. The loading and extension data were measured and recorded. The generated test result reports were used to determine the tensile properties, and uniaxial tension behaviours, which were used in the establishment of the FLDs.

2.2. Erichsen cupping test experiments

Two sets of AA6082-O square shells (60 mm × 60 mm) deep drawing specimens (1.0 mm and 2.0 mm, 5 specimens per thickness per set) were prepared. Gridlines with an offset of 10 mm, and a total of 5 concentric circles were printed on the surface of the test specimens prior to the onset of loading. These circles share the same centre with the test specimen (see Fig. 8). Four points were marked on the circumference of the circles, two points along

the vertical and two points along the horizontal centreline of the scribed circles.

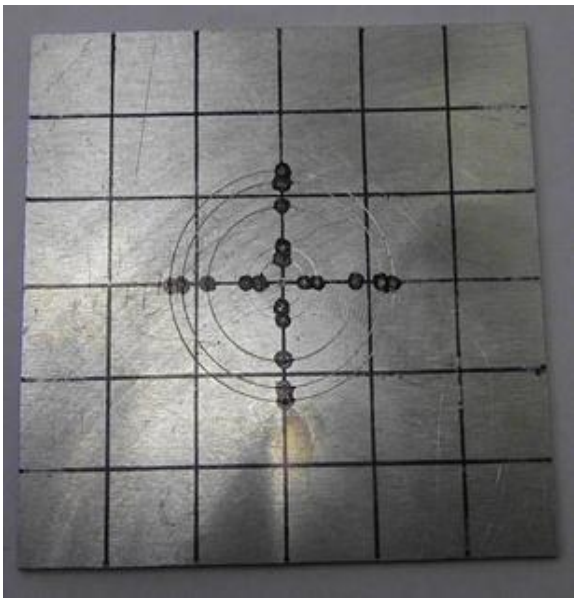


Fig. 8: Circle Grid Print on the Deep Drawing Test Specimens.

The diameters (initial diameters) of the 5 concentric circles, starting from the inner circle (smaller circle) were: 5 mm, 8 mm, 17 mm, 23 mm and 27 mm, respectively. A circle stencil, a metal scriber and an adjustable divider were used to scribe these gridlines and circles on the surface of the Erichsen cupping test specimens before the tests.

To generate uniaxial, biaxial and equiaxial tension conditions, four of the five (4/5) test specimens were cut to two distinct geometries (SG1 and SG2), as seen in Fig. 9, with two test specimen samples per test geometry, and per test thickness. A leverage sheet metal shear was used to create the notches or grooved segments, to establish the desire geometries. The fifth test specimen was prepared with no notches/grooved segments (SG0), as seen in Fig. 9, per each test thickness. These two specimens were used for the control of experiments for each test thickness.

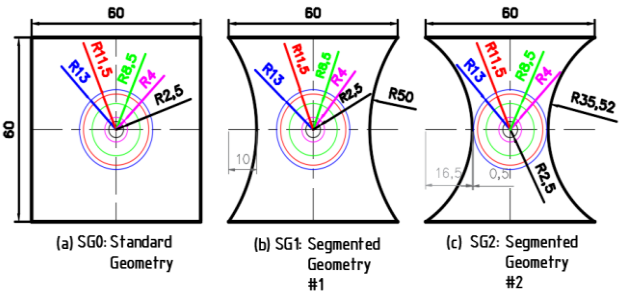


Fig. 9: Erichsen Cupping Test Specimen Geometries.

The dimensions of the created notches or grooved segment geometries (segment width × height × groove radius) were:

a) SG0: Un-grooved (no notches)
b) SG1: 60 × 10 × (48.5 ±1.50
c) SG2: 60 × 10 × (34.0 ± 1.52)

Upon the establishment of the desired geometries, the 20 mm spherical punch, 27 mm die and the inscribed surface of the specimens were lubricated with Vaseline BLUESEAL jelly. Afterward, the specimen to be tested was centrally mounted on the die and clamped tightly between the die and the holding clamp using two hexagonal bolts. The prepared body was then set on the Universal Material Tester (the same machine used for the tensile test experiments), through the tube of the compression zone of the machine, and the drawing punch gently pressed against the specimen by means of the hydraulic device using screw hand wheel on the master cylinder, until a crack appeared on the budge dome (the mirror). The penetration depth of the punch onto the surface of the specimens was measured with a Vernier depth gauge, upon unloading, which gave the Erichsen Index (IE) of the drawn part.

After the deep drawing process the distances between the two marked points on each circle's vertical and horizontal centreline were measured and recorded as minor and major diameters of the distorted circles. These measurements were used in the determination of the minor and major strains, and in the establishment of the Forming Limit Diagrams.

3. Results and discussion

3.1. Uniaxial tensile test

The tensile-test specimens fractured with little or no observable necking, as evident in Fig. 10.

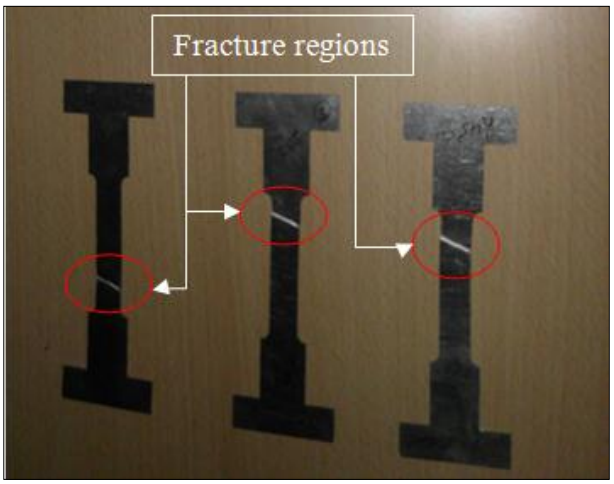


Fig. 10: Fractured Tensile-Test Specimens.

Stretcher-strain marks (Lüders bands) were observed on the test specimens cut at 90^0 to the rolling direction, starting from the top (front) end of the specimen and propagating downward, as the specimens were being loaded. The formed bands were observed to be positively inclined (at an angle approximately $\geq 45^o$, relative to the axis of the specimen). This phenomenon is only common to low-carbon-steels and other polycrystalline body-centred cubic (bcc) metals, and to certain aluminium – magnesium (Al – Mg) alloys [33]. Thus it could be that AA6082-O alloy is one of the few Al-Mg alloys with non-uniform yielding characteristics.

3.1.1. Stress-strain behavior

It is evident from Fig. 11 that the alloy's stress-strain behaviour resembles that of a typical aluminium metal, with the characteristic curve showing high formability and moderate tensile strength. The specimens cut at 0^o to the rolling direction exhibited the highest yield strength, tensile strength, and modulus of elasticity at both thickness levels. However, the ductility of the 1.0 mm thick specimens was lower than of the 2.0 mm thick specimens at the respective angular orientations. This is in agreement with [5], who discusses the effect of thickness and angular orientation on sheet properties.

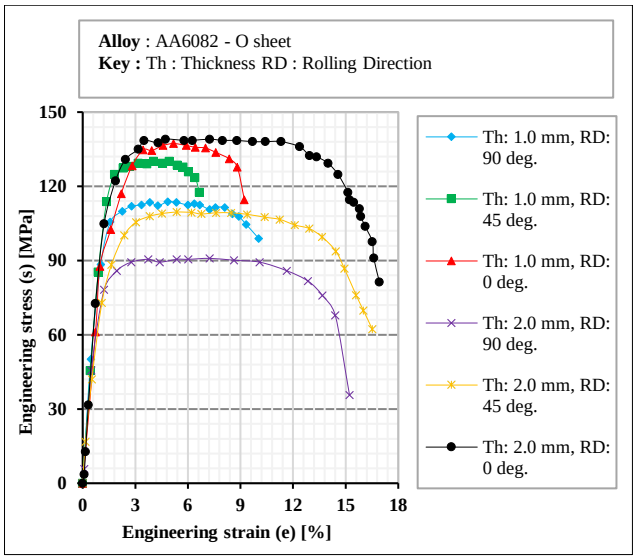


Fig. 11: AA6082-O Stress-Strain Behaviour.

3.1.2. Tensile properties

Tensile properties of tested specimens are listed in Table 3:

Table 3: Obtained Tensile Properties

Thickness	Orientation	UTS (MPa)	YS (MPa)	E (GPa)	El [%]
	0º	138.57	82.11	88.33	12.37
1.0 mm	45º	130.13	85.39	85.09	11,92
	90º	113.77	88.46	83.64	11.56
	0º	139.08	72.61	89.60	16.93
2.0 mm	45º	109.60	72.86	64.48	16.52
	90º	90.89	78.23	53.39	15.22

The tensile strengths for 1 mm thick specimens were consistently higher than for the 2 mm thick specimens for all three orientations. However, only the tensile strengths in the rolling direction for both thicknesses approximate the value given by [8]. On the basis of the ductility (% Elongation) the formability of this alloy is highest in the rolling direction, and enhanced by increased sheet thickness. The variability in the yield strengths at different orientations suggests the alloy exhibits anisotropic behaviour due to texturing. In summary:

a) $[UTS, E, \%EL]_{0^o} > [UTS, E, \%EL]_{90^o}$;
b) $[UTS, E, \%EL]_{45^o} > [UTS, E, \%EL]_{90^o}$;
c) $[UTS, E, \%EL]_{2.0\ mm} > [UTS, E, \%EL]_{1.0\ mm}$;
d) $YS_{90^o} > YS_{45^o} > YS_{0^o}$; and
e) $YS_{1.0\ mm} > YS_{2.0\ mm}$.

3.1.3. Strain hardening exponent, n

After applying a logarithmic operation on the Holloman-Ludwig equation, the strain hardening exponent (n) values were determined from the log σ – log ε plot for the strain range of 0.05 % - 0.7 %, as shown in Fig. 12. The corresponding strength coefficients (K-values) were also determined using the Holloman-Ludwig equation.

It can also be observed from Fig. 12 that the formability of the alloy is highest in the rolling direction than in the transverse direction and 45º orientation, and increases with an increased sheet thickness. In summary:

a) $n > 1$;
b) $n_{0^o} > n_{45^o} > n_{90^o}$; and
c) $n_{1.0\ mm} > n_{2.0\ mm}$

The n-values lie in the range 1.55 - 1.81. Thus the aluminium AA6082-O alloy has a higher range of n-values than those ($0.02 \leq n \leq 0.51$) of comparable ductile metals. In general, an increase in the n-value corresponds to an increase in an alloy's resistance to necking and indeed the tensile test specimens fractured without necking. A perfectly plastic material would have an n-value of 0 while a perfectly elastic material would have an n-value of 1, so the aluminium AA6082-O alloy deviates from the norm in this regard. However n-values far exceeding unity have been calculated for stainless steels using modified Ramberg-Osgood models [35]. A study on the deformation characteristics of $Al_{70}Pd_{21.5}Mn_{8.5}$ poly-quasicrystals yielded n-values of 1.2 ± 0.2 [36]. Thus the AA6082-O alloy chemical composition could reasonably account for the n-values obtained in this study. According to a study on intermetallic phase particles in a 6082 aluminium alloy [37], the as-cast microstructure consisted of seven phases, namely: α-Al, β-Al_5FeSi, α-AlFeSi, α-$Al_{15}(FeMn)_3Si$, Al_9Mn_3Si, Mg_2Si and Si between the aluminium dendrites. The major disadvantage of intermetallics is their low ductility, especially at low and transitional temperatures. But heat treatment procedures, chemical solutions and microstructural control can be used to improve the mechanical properties of such alloys [38].

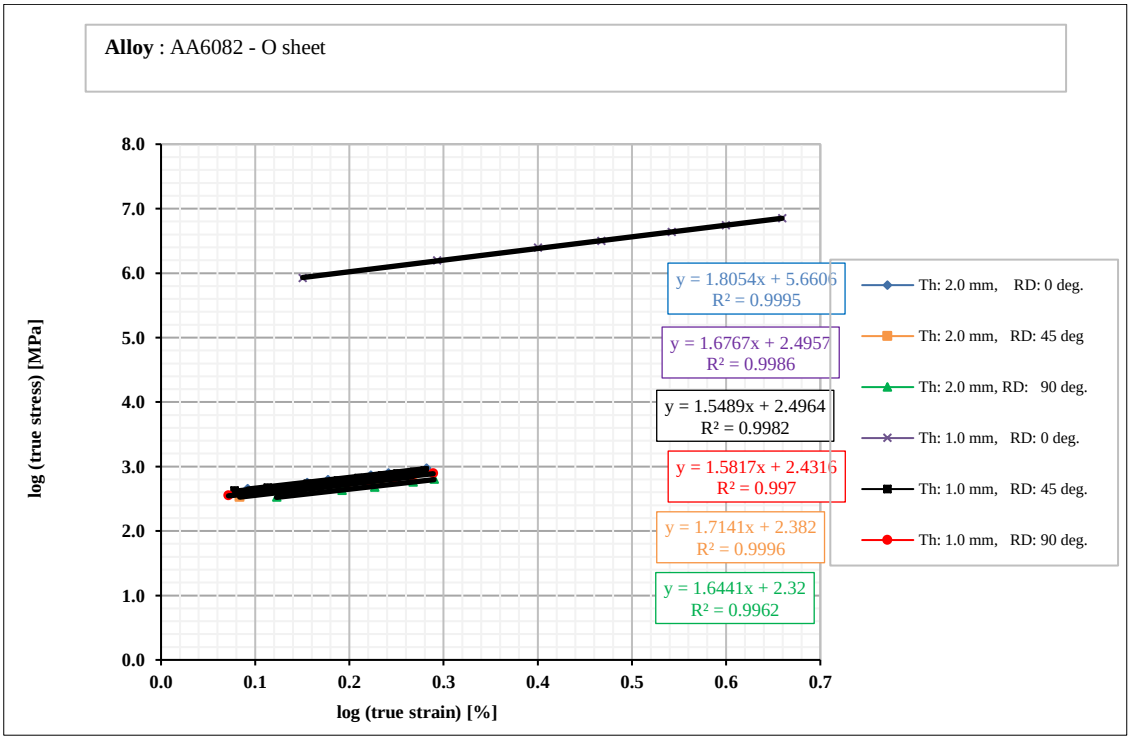


Fig. 12: Strain Hardening Exponent Determination by the Holloman-Ludwig Equation (Log Σ – Log E Plot).

3.1.4. Plastic strain ratios

The computed plastic anisotropy ratios and n-values are listed in Table 4.

Table 4: Plastic Anisotropy Ratios and N-Values

Thickness	Orientation	r	R-value	r_{ave}	Δr	$n_{(2-6)\%}$	K [MPa]
1.0 mm	0°	0.75	0.56	0.59	-0.20	1.68	63.89
	45°	0.69				1.55	35.39
	90°	0.23				1.58	38.17
2.0 mm	0°	2.40	1.99	2.06	-0.44	1.81	47.50
	45°	2.28				1.71	51.77
	90°	1.28				1.64	44.07

In the same manner as the tensile properties and n-values, it is clear from Table 4 that the obtained r-values also indicated that the formability of AA6082-O sheet is highest in the rolling direction and enhanced by increased thickness.
This is evident from a combination of the following parameters:

a) $[r, R, r_{ave}, n]_{2.0\ mm} > [r, R, r_{ave}, n]_{1.0\ mm}$;
b) $[n_{2.0\ mm} > n_{1.0\ mm} > 1]$;
c) $[R_{2.0\ mm} > R_{1.0\ mm} > 0.5]$;
d) $[r_{ave}]_{2.0\ mm} > [r_{ave}]_{1.0\ mm} \geq 0.5$; and
e) $[r_o > r_{45} > r_{90}]_{2.0\ mm} > [r_o > r_{45} > r_{90}]_{1.0\ mm}$
f) $[\Delta r_{2.0\ mm} \leq -0.44] < [\Delta r_{1.0\ mm} \leq -0.20]$

Since all Δr values are negative, aluminium AA6082-O alloy is susceptible to earing (Figs. 13-14) during deep drawing operations.

3.2. Erichsen cupping tests

3.5.1. Deep drawn specimens

The deep drawn parts demonstrated the differentiation of strain state behaviour of the AA6082-O sheet metal, and possible deep drawing defects that can be encounter during deep drawing operations with this alloy. It was observed that some of the concentric circles deformed into ellipses. This is evident only from the tested specimens with notches/grooved segments (see Fig. 13):



Fig. 13: Drawn Specimen (2.0 Mm) with Deformed Circles.

It was also observed during the test that less force is required to cause the inward flow of material from the sides of the test specimens for the thinner sheet metals (1.0 mm) than for the thicker sheet metals (2.0 mm). This is evident from the differences in height (IE) of the drawn parts of the two thickness.
It was further observed that insufficient clamping force results in excessive inflow of materials into the die cavity. This is evident from the location of the two ears formed on the top section of the drawn shells. These ears are all located on the notched/grooved sections. It was also observed that the total number of the formed ears is always in multiples of 2.

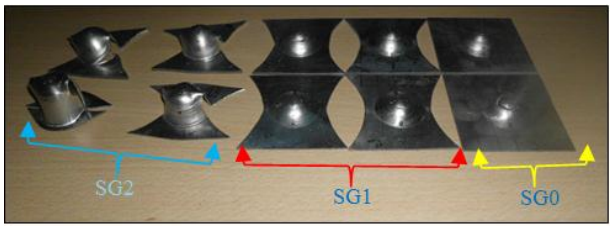


Fig. 14: Deep Drawn Specimens.

3.5.2. Breaking force, limiting drawing ratio and Erichsen index number

Upon the unloading and completion of the experiments the average Breaking Force (BF), the Punch penetration depth or Erichsen Index number (IE) and Forming Drawing Ratio (LDR) were determined as listed in Table 5, and their relationship indicated in Fig. 15.

Table 5: Average Breaking Force (BF), Erichsen Index Number (IE) and Limiting Forming Drawing Ratio (LDR)

Indicative Parameters	Specimen Geometry (SG) and Thickness					
	SG0		SG1		SG2	
	1.0 mm	2.0 mm	1.0 mm	2.0 mm	1.0 mm	2.0 mm
BF_{ave} [kN]	2.7	7.40	3.50	7.79	6.23	8.7
IE_{ave}	7.5	10.6	7.14	11.2	14.3	17.7
LDR_{ave}	3.0		2.0		1.35	

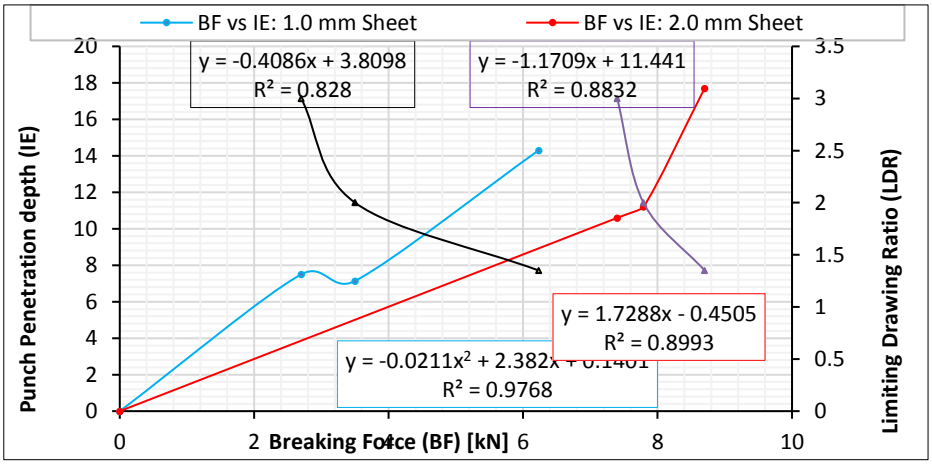


Fig. 15: The Relationship between BF, IE and LDR.

It is evident from Table 5 and Fig. 15 that as practically reasonable greater loads (BF) are required when forming thicker metal sheets than thinner metal sheets of the same type and grade. However, it can be inferred from Fig. 15 that as the cup depth (IE-value) increases or material is thin (1.0 mm) there is an increased tendency for forming defects (due to the resultant lower LDR-value < 2.0).

Moreover, it is clear from Table 5 and from the formula for determining the LDR-value that the material thickness does not have any significant effect on the obtained LDR-values. Thus, the LDR-value obtained for the SG0-geometry ($LDR_{SG0} = 3.0$) is more of a material parameter than a geometric parameter, but the opposite is very true for the LDR-values obtained for SG1 and SG2-geometries ($LDR_{SG1} = 2.0$ and $LDR_{SG2} = 1.35$. Thus it could be inferred that AA6082-O alloy has the best drawability ($LDR_{SG0} = 3.0$)). Thus, better formability in forming AA6082-O, alloy without occurrence of earing defects, is only attainable with $LDR > 2.0$.

3.5.3. Deep drawing defects

Observed defects included earing, tearing, surface scratches and excessive thinning. These defects are presented in Fig. 16-18. The earing is a material property defect, which resulted from the anisotropic properties of AA6082-O alloy. The differences in the height of the formed ears are greatly influenced by the blanking geometry; whereas the rest of the other encountered defects (tearing, excessive thinning and surface scratches) are forming process defects. Tearing and excessive thinning are due to high tensile stresses, resulting from either excessive loading force or too high blank holding pressure or a combination of the two. On the other hand, the scratches on the drawn parts are a tooling parameter defect, resulting from the tribology of the tooling used (surface condition of the sheet, and the roughness of the punch and die).



Fig. 16: Earing And Scratching.

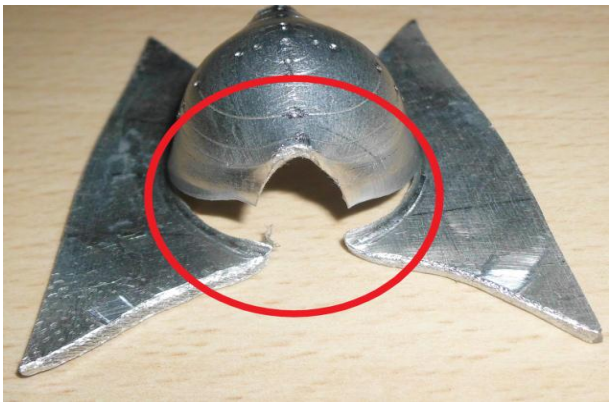


Fig. 17: Tearing, Excessive Thinning, and Earing.

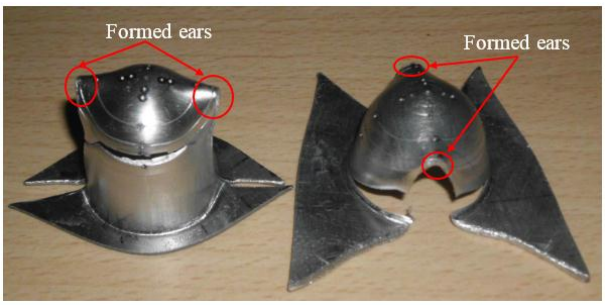


Fig. 18: Earing, Tearing, and Excessive Thinning.

3.5.4. Forming limit curves (FLCs) and forming limit diagrams (FLDs)

The FLCs and FLDs of the alloy were established from pairs of Forming Limit strain ($\varepsilon_1, \varepsilon_2$) values obtained for various loading paths, as indicated in Fig. **19**. It is evident from the established FLC levels that the formability of AA6082-O is enhanced by an increasing sheet metal thickness.

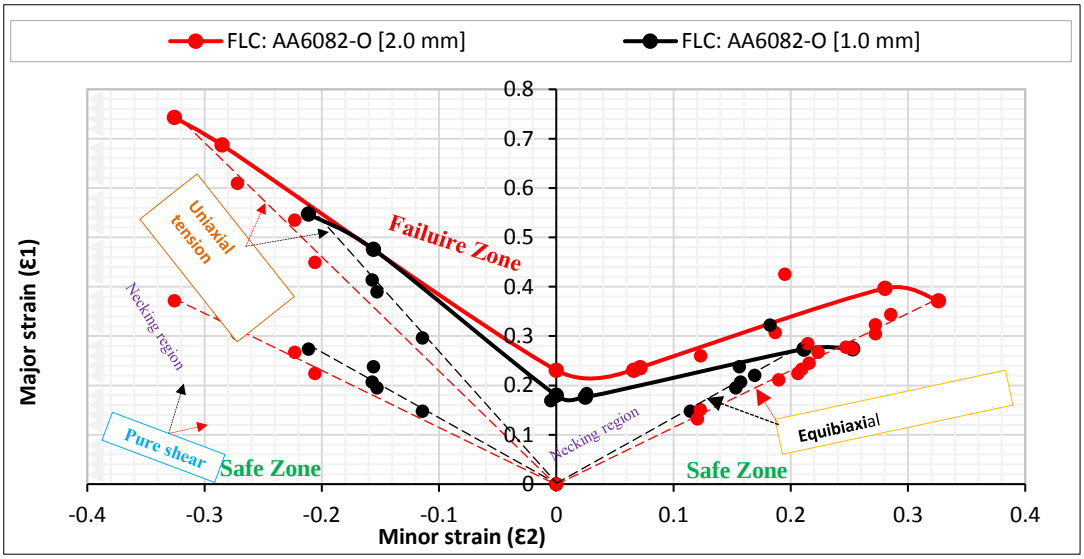


Fig. 19: Strain Measurements and FLD of AA6082-O Sheet Metal.

The FLCs for the two thicknesses (1.0 mm and 2.0 mm) do not fall within one universal band; however they have similar orientation and shape. Since the FLC for the 2.0 mm thickness is higher than the other one, it implies the formability of the alloy increases with an increase in sheet thickness.

The major strain (ε_1) and minor strain (ε_2) values obtained by varying the blank thickness and groove size on the blank during the Erichsen cupping tests were consistent and fell along the positive minor strain (ε_2) axis as predicted by Keeler [14, 26, 29, 31]. The shape and size of the grooves on the test specimens strongly influenced the strain paths (distribution).

4. Conclusions

Based on the Uniaxial Tensile test experiments conducted; it is inferred that aluminium AA6082-O alloy's stress-strain behaviour resembles that of other aluminium alloys in the 6000 series. The alloy fractures with little or no observable necking when subjected to uniaxial tension, which denotes brittleness. It exhibits non-uniform yielding characteristics (Lüders band formation and propagation), a phenomenon which is only common to low carbon-steel alloys, and certain Al-Mg alloys.

The alloy also exhibits planar anisotropy characteristic ($\Delta r < 1$), hence, is susceptible to earing defects in deep drawing forming operations, especially when the Limiting Drawing Ratio of the test material is less than 3.0 ($LDR < 3$).

The tensile strength of aluminium AA6082-O alloy is typically highest in the rolling direction (0^0), and enhanced by increased sheet thickness. Thus the formability increases with sheet thickness characterised by strain hardening exponent values and strain ratios of $n > 1$ and $r > 0.5$ respectively. The alloy exhibits a triple n-behaviour ($n > 1 > 0.5$), but the formability is higher in the rolling direction compared to the transverse directions.

Moreover, based on the Erichsen Cupping test experiments, the Forming Limit Curve levels of the established FLDs of AA6082-O alloy elevates with increased sheet thickness ($FLC_{2.0mm} > FLC_{1.0mm}$). Thus, this gives further evidence that the formability of AA6082-O alloy is enhanced by increased sheet thickness, when the test material is subjected to uniaxial, biaxial and equi-axial tension conditions in deep drawing operations.

Although it is normal with the Holloman-Ludwig equation to obtain n -values greater than unity, the obtained n -values ($1.55 \leq n_{AA6082-O} \leq 1.81$) are much higher (about 55%) than the commonly known n-values ($n_{normal} \leq 1$), and triple those of the comparable brittle metals and aluminium alloys ($0.02 \leq n_{comparable} \leq 0.5$, at room temperature). Hence further work is required to clarify and confirm the range of the n-values of this alloy (AA6082-O), by using:

1) Numerical simulative methods, applying other equations such as the Ramberg-Osgood models together with the Holloman-Ludwig equation used in this study, and comparing the resultant n-values; or
2) Simulation software; or
3) Circular shell test specimens, with smaller grid circle prints, and testing on same equipment; or
4) Different testing equipment.

Acknowledgements

This work was accomplished with support from the Department of Mechanical and Industrial Engineering, University of Namibia and the Namibia Training Authority (NTA). We also appreciate Jinan Precision Equipment CO. LDT, from People's Republic of China for supplying the aluminium AA6082-O sheet metal test samples.

References

[1] Benhabib B, Manufacturing: Design, Production, Automation, and Integration, Marcel Dekker Inc., New York, NY, (2003), p. 216. https://doi.org/10.1201/9780203911204.

[2] Subramonian S & Kardes N, "Materials for Sheet Forming," Sheet Metal Forming: Fundamentals, ASM International, (2012), p. 73.

[3] Nghishiyeleke ET, "An evaluation of the deep drawability of aluminium AA6082-O sheet," Unpublished Thesis, (2015).

[4] Heinzel H & Neitzert T, "Forming of locally made sheet steels - Issues and Opportunities," HERA, available online: http://slideplayer.com/slide/3836809/, last visit: 16.09.2018.

[5] Gedney R, "Measuring the plastic strain ratio of sheet metals: A useful fool for evaluating material", The FABRICATOR, (2006), available online: https://www.admet.com/wp-content/uploads/2015/12/june_06_FAB.pdf, last visit: 16.09.2018.

[6] Sarna SK, "Defects in Thermo Mechanical Processing of Metals," Ispat Digest, (2016), available online: http://ispatguru.com/defects-in-thermo-mechanical-processing-of-metals/. last visit: 05.10.2018.

[7] SIMTECH, "Introduction to Sheet Metal Forming Processes," SimTech Simulation et Technologie, (2001), available online: http://www.simtech.fr/pdfS/IntroToSheetMetalFormingProcesses.pdf, last visit: 22.07.2018.

[8] "6082-O Aluminum," MakeItFrom.com, (2017), available online: https://www.makeitfrom.com/material-properties/6082-O-Aluminum. last visit: 15.08.2017.

[9] "Aluminium Alloy 6082 Material Data Sheet," Thyssenkrupp Materials (UK) Ltd, (2016), available online: https://www.thyssenkrupp-materials.co.uk/media/material_data_sheets/aluminium/aluminium_alloy_6082_nb.pdf, last visit: 25.04.2018.

[10] Davis JR, ASM Materials Engineering Dictionary, ASM International, Novelty, OH, (1992), pp.485-512.

[11] Pfeifer M, "Sheet Metal Formability," Industrial Metallurgists, LLC., (2014). available online: https://www.imetllc.com/sheet-metal-formability/. last visit: 17.09.2018.

[12] Gedney R, "Sheet Metal Testing Guide: Formability of Sheet Metals, Measuring the Plastic Strain Ratio of Sheet Metals, Tensile Testing for Determining the Formability of Sheet Metals," ADMET Inc., Norwood, (2013).

[13] Niemeier BA, Schmieder AK & Newby JR, Formability Topics-Metallic Materials, American Society for Testing and Materials (ASTM), Baltimore, Md. (1978), pp. 39-150. https://doi.org/10.1520/STP647-EB.

[14] Banabic D, Bunge HJ, Pohlandt K, & Tekkaya AE, "Main tests used to determine the FLD," Formability of Metallic Material: Plastic anisotropy, Formability Testing, Forming Limits, Springer, (2000). https://doi.org/10.1007/978-3-662-04013-3.

[15] Eric K & Danny S, "The Formability of sheet metals," AutoForm Blog, (2016). available online: https://www.autoform.com/blog/material-matters-knowing-your-limit/. last visit: 17.09.2018.

[16] Zhou H & Attard TL, "Simplified Anisotropic Plasticity Model for Analyzing the Post yield Behavior of Cold-Formed Sheet-Metal Shear Panel Structures," Journal of Structural Engineering, Vol. 141, No. 7, (2015), p. 4014185, available online: last visit: 18.09.2018. https://doi.org/10.1061/(ASCE)ST.1943-541X.0001152.

[17] Davis JR, Semiatin SL, & American Society for Metals, ASM Metals Handbook, Vol. 14: Forming and Forging, ASM International, (1989). pp. 888 – 897.

[18] Truszkowski W, "Strain Ratio as the Measure of Plastic Anisotropy," The Plastic Anisotropy in Single Crystals and Polycrystalline Metals, Kluwer Academic Publishers, (2001), pp. 19-36, available online: last visit: 12.11.2018. https://doi.org/10.1007/978-94-015-9692-3_3.

[19] Youssef HA, El-Hofy HA & Ahmed MH, Manufacturing Technology: Materials, Processes, and Equipment, CRC Press, (2012), pp 175-292.

[20] Henry S, Sanders B, Palakowski C, & Pace P, "Description of test material," Tensile Testing, 2nd edn, ASM International, (2004), p. 49.

[21] ISO, "ISO 20482:2013: Metallic materials -- Sheet and strip -- Erichsen cupping test," International Organization for Standardization, (2013), available online: https://www.iso.org/standard/63857.html. last visit: 17.09.2018.

[22] Kalpakjian S & Schmid S, Manufacturing Engineering and Technology, Prentice Hall, New York, NY, (2010), pp. 381 - 431.

[23] Venkatachalam G, Patel Nilay S, Mishra D, Singh S, Choudhary Y & Narayanan S, "Determination of Forming Limit Diagram for Perforated Aluminium 1050A Sheets", International Journal of Mechanical & Mechatronics Engineering, Vol. 13, No. 01, (2013), pp. 37-39.

[24] Yeh FH, Li CL & Tsay KN, "An Analysis of Forming Limits for Various Arc radii of Punch in Micro Deep Drawing of the Square Cup", Advanced Materials Research, Vol. 433-440, (2012), pp. 660-665, available online last visit: 04.12.2018. https://doi.org/10.4028/www.scientific.net/AMR.433-440.660.

[25] Talič-Čikmiš A, Pepelnjak T, & Hasnbegovič S, "Experimental Determination of Forming Limit Diagram", Proceedings of the 14th Internation Research/Expert Conference on Trends in the Development of Machinery and Associated Technology, (2010), pp. 605-608, available online: https://www.tmt.unze.ba/zbornik/TMT2010/152-TMT10-054.pdf, last visit: 04.12.2018.

[26] Tisza M, & Kovács ZP, "New Methods for Predicting the Formability of Sheet Metals", Production Processes and Systems, Vol. 5, No. 1, (2012), pp. 45-54, available online: http://phd.lib.uni-miskolc.hu/JaDoX_Portlets/ documents/document_13400_section_5558.pdf, last visit: 04.12.2018.

[27] Todkar SS, Chhapkhane NK, & Todkar SR, "Investigation of Forming Limit Curves of Various Sheet Materials using Hydraulic Bulge Testing with Analytical, Experimental and FEA Techniques", International Journal of Engineering Research and Applications, Vol. 3, No. 1, (2013), pp. 858-863.

[28] Banabic D, Dragos G, & Bichis I, "Influence of Variability of Mechanical Data on Forming Limits Curves", Metal Forming, Vol. 3, No. 1, (2013), pp. 858-863

[29] Chen J & Zhou X, "A New Curve Fitting Method for Forming Limit Experimental Data", Journal of Materials Science and Technology, Vol. 21, No. 4, (2005), pp. 521-525.

[30] Son H, "Calculations of Forming Limit Diagrams for Changing Strain Paths on the Formability of Sheet Metal", Journal of Material Science & Technology, Vol. 17, No. 1, (2001), pp. 141-142.

[31] Balod AE, Hadi MH & Basher EA, "The Effect of Load Punch in the Limits of Strain Paths for (1006) Steel Sheets by using Stretch Forming", Anbar Journal for Engineering Sciences, Vol. 21, No. 4, (2005), pp. 102-108.

[32] Kim SB, Huh H, Bok HH, & Moon MB, "Forming Limit Diagram of Auto-Body Steel Sheets for High-Speed Sheet Metal Forming", Journal of Materials Processing Technology, Vol. 211, No. 5, (2011), pp. 851-862, available online. last visit: 04.12.2018. https://doi.org/10.1016/j.jmatprotec.2010.01.006.

[33] Roxana H, Lynann C & Rogge R, "Intergranular Strain and Texture in Steel Lüders Bands," Acta Materialia, Vol. 53, No. 12, (2005), pp. 3517-3524. https://doi.org/10.1016/j.actamat.2005.04.008.

[34] Sekhara RAC & Kumar TP, "Forming Limit Diagram for Sheet Metal Forming: Review", International Journal of Advance Research and Innovative Ideas in Education, Vol. 2, No. 2, (2017), pp. 155-162, available online: http://ijariie.com/AdminUploadPdf/Forming_Limit_Diagram_for_Sheet_Metal_Forming__Review_1496.pdf. last visit: 04.12.2018.

[35] Arrayago I, Real E & Gardner L, "Description of stress-strain curves for stainless steel alloys," Materials and Design, Vol. 87, (2015), pp. 540-552, available online:https://core.ac.uk/download/pdf/77020953.pdf. last visit: 05.06.2019.

[36] Hirth JP, Dislocations in Solids: A Tribute to F.R.N. Nabarro, Vol. 14, Elsevier, (2011), pp. 251 – 331.

[37] Mrówka-Nowotnik G, Sieniawski J & Wierzbiñska M, "Intermetallic phase particles in 6082 aluminium alloy," Archives of Materials Science and Engineering, Vol. 28, No. 02, (2007), pp. 69 – 76. available online: http://www.amse.acmsse.h2.pl/vol28_2/2821.pdf. last visit: 06.06.2019.

[38] Ebhota WS & Jen TC, "Intermetallics Formation and Their Effect on Mechanical Properties of Al-Si-X Alloys," Intermetallic Compounds - Formation and Applications, IntechOpen, (2018), pp. 21-41, available online: https://www.intechopen.com/books/intermetallic-compounds-formation-and-applications/intermetallics-formation-and-their-effect-on-mechanical-properties-of-al-si-x-alloys. last visit: 06.06.2019.